EXPERIMENTAL DESIGN FOR VALIDATING RELATIVISTIC PONDEROMOTIVE DYNAMICS VIA LASER MODULATION OF MeV ELECTRON BEAMS*

J. Zhang, G. Feng, Z. He†, Y. He, X. Xu, F. Zhang, H. Zhang, J. Chen,
National Synchrotron Radiation Laboratory,
University of Science and Technology of China, Hefei, China

Abstract

We present a design for the experimental validation of relativistic ponderomotive dynamics on a realistic MeV electron-beam platform. The scheme combines an S-band gun with a co-propagating focused laser pulse to induce longitudinal momentum modulation in relativistic electrons. Using a non-paraxial laser-field model and beam-dynamics simulations, we evaluate the expected post-interaction energy signatures and their observability on a practical beamline. Particular attention is given to the dependence of the modulation on laser focusing, beam parameters, and synchronization errors. The analysis identifies the dominant force contributions governing the final energy distribution. These results provide a practical route for translating previously derived relativistic ponderomotive theory into a testable experiment.

INTRODUCTION AND OBJECTIVE

In previous work, relativistic ponderomotive dynamics in focused laser fields were derived analytically [1–3]. The present study addresses the next step required for experimental validation, namely the translation of that theoretical framework into a practical beamline configuration with realistic MeV electron-beam and laser parameters.

The proposed scheme is based on an S-band electron gun and a co-propagating focused laser pulse, with the aim of generating a measurable longitudinal momentum modulation in a relativistic electron bunch. In this context, the relevant question is whether the corresponding post-interaction energy signature can be resolved under realistic operating conditions, including finite emittance, energy spread, focusing constraints [4, 5], as well as laser–electron interaction effects and relativistic ponderomotive response [6, 7].

The objective of this paper is therefore to establish a parameterized validation scheme for relativistic ponderomotive dynamics. A realistic experimental layout is defined, the corresponding observables are identified, and the expected modulation signatures are evaluated by means of field-based beam-dynamics simulations.

THEORETICAL BASIS AND VALIDATION PRINCIPLE

The on-axis longitudinal ponderomotive response in a focused traveling-wave laser field was derived in the laboratory frame as

$$F_{p,z}^{(\mathrm{theory})} \simeq -\frac{q^2}{2m}\left[\frac{1}{\gamma_0(\omega-kv_{0z})^2}\partial_z\langle E_z^2\rangle - \frac{2\langle E_z^2\rangle}{\gamma_0^2(\omega-kv_{0z})^3}\partial_z\Omega_{\mathrm{OC}}\right], \qquad (1)$$
$$\Omega_{\mathrm{OC}} = \gamma_0(\omega-kv_{0z}),$$

where $\langle E_z^2\rangle$ is the cycle-averaged squared longitudinal field on axis and Ω_{OC} is the Doppler-shifted carrier frequency in the oscillation-center frame. Eq. (1) is the primary theoretical quantity from which the present validation scheme is constructed [1, 8, 9].

However, the applicability of Eq. (1) is itself conditional, because it relies on the cycle-averaged description of the laser–electron interaction [3, 10]. This validity is governed by the effective number of optical cycles experienced by the electron within the interaction region,

$$N_{\mathrm{eff}} \simeq \frac{|\Delta\Phi|}{2\pi} = \frac{2\pi w_0^2}{\lambda^2}\frac{1-s\beta_e}{\beta_e} - \frac{1}{4}, \qquad (2)$$

where w_0 is the focal waist, λ is the laser wavelength, $\beta_e = v_{0z}/c$, and $s = 1$ and $s = -1$ correspond to co-propagating and counter-propagating geometries, respectively. The condition $N_{\mathrm{eff}} \geq N_{\mathrm{min}}$ then defines a critical beam waist, analogous to phase-slippage and finite-interaction-length effects in laser–electron interactions [11],

$$w_0^{\mathrm{crit}} = \sqrt{\frac{(N_{\mathrm{min}}+1/4)\,\lambda^2\beta_e}{2\pi(1-s\beta_e)}}, \qquad (3)$$

which separates the multi-cycle regime, where cycle averaging is reliable, from the near-critical and sub-cycle regimes, where phase-dependent effects become increasingly important [1].

This point determines the validation strategy adopted in the present work. The experiment is not designed merely to detect a nonzero downstream energy change, but to test whether the observed beam response evolves with w_0 in the manner predicted by Eqs. (2) and (3). In other words, the quantity to be validated is not only the longitudinal ponderomotive response itself, but also the transition between interaction regimes controlled by the laser waist. The critical waist therefore becomes the central physical concept linking the theory to the experiment.

The final diagnostic is a downstream magnetic spectrometer, since the force in Eq. (1) cannot be measured directly.

* Work supported by the National Key Research and Development Program of China (Grant No. 2024YFA1612200).
† hezhg@ustc.edu.cn

Under nominal symmetric interaction conditions, the most relevant observables are the laser-induced spectral broadening and the associated spectral reshaping, quantified for example through

$$\Delta\sigma_E = \sigma_{E,\mathrm{on}} - \sigma_{E,\mathrm{off}}, \tag{4}$$

where the subscripts "on" and "off" denote measurements with and without laser interaction. By contrast, the centroid shift

$$\Delta E_c = \langle E \rangle_{\mathrm{on}} - \langle E \rangle_{\mathrm{off}} \tag{5}$$

is treated here as a secondary observable, since a nonzero ΔE_c is expected to be more sensitive to timing offset, synchronization jitter, and asymmetric beam–laser overlap than to the nominally symmetric ponderomotive response itself [12].

Accordingly, the validation criterion adopted here is twofold. First, the final electron spectrum must show a measurable and reproducible modification induced by the focused laser field. Second, the dependence of this spectral response on w_0 must remain consistent with the regime structure predicted by the effective-cycle analysis, namely a cycle-averaged response for $w_0 \gg w_0^{\mathrm{crit}}$, a transition region for $w_0 \sim w_0^{\mathrm{crit}}$, and increasingly non-ideal or phase-sensitive behavior for $w_0 < w_0^{\mathrm{crit}}$.

EXPERIMENTAL LAYOUT AND WAIST-SCAN STRATEGY

The proposed setup consists of an S-band electron gun, a solenoid-based transport section, a laser–beam co-propagation region formed by an off-axis parabolic (OAP) mirror, and a downstream magnetic spectrometer followed by a screen [4, 5]. The laser pulse is generated by an 800 nm laser system and is focused by the OAP mirror into the interaction region [13–15]. The relativistic electron bunch is transported and focused by the solenoid such that the electron-beam focus is spatially overlapped with the laser focus. The schematic layout is shown in Fig. 1. The downstream electron energy spectrum is then measured with the laser switched on and off under otherwise identical machine conditions.

The role of the beamline is not simply to realize a generic laser modulation experiment, but to provide a controlled scan of the key theoretical parameter w_0/w_0^{crit}. The central experimental variable is therefore the focused laser waist w_0. In the present setup, w_0 is adjusted through the input beam size on the off-axis parabolic mirror. For a Gaussian beam focused by an OAP with focal length f, the waist can be estimated as

$$w_0 \simeq \frac{2\lambda f}{\pi D_{\mathrm{in}}}, \tag{6}$$

where D_{in} is the incident laser-beam diameter on the OAP. By changing D_{in} while keeping the beam energy and carrier wavelength fixed, the interaction can be moved systematically from the multi-cycle regime into the near-critical regime [16]. Eq. (6) provides the nominal diffraction-limited

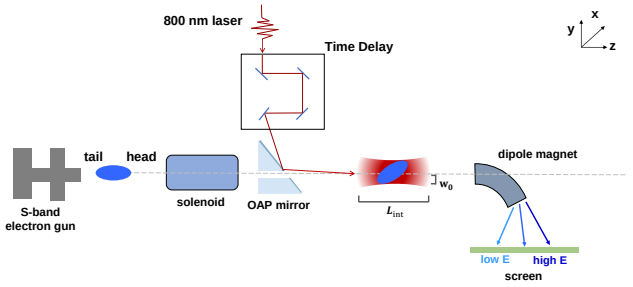

Figure 1: Schematic layout of the proposed experiment for validating relativistic ponderomotive dynamics. The laser–beam interaction takes place over an effective interaction length L_{int} near the laser waist w_0.

waist and is used here as the reference relation between the optical setup and the theoretical control parameter.

The baseline parameter setup is defined by two groups of quantities. The first group contains the electron-beam parameters of the practical platform, including beam energy, bunch charge, rms bunch length, normalized emittance, transverse beam size at the interaction point, and initial rms energy spread. These quantities determine the intrinsic spectral width against which the laser-induced response must be resolved. The second group contains the laser and overlap parameters, including carrier wavelength, pulse duration, focal waist, focal position, peak field amplitude, and relative beam–laser timing. Together, they determine both the magnitude of the longitudinal modulation and the regime in which the interaction takes place.

The nominal operating point is chosen such that the laser-induced spectral modification remains measurable while the interaction still lies within, or near, the cycle-averaged validity window predicted by the theory. In practice, the validation is based on a reference configuration with approximately symmetric overlap, followed by a controlled waist scan across the predicted critical region. The primary comparison is therefore not a single-shot spectrum, but the trend of the downstream spectral response as a function of w_0 relative to w_0^{crit} [1]. Other key parameters are shown in Table 1.

NUMERICAL IMPLEMENTATION, PREDICTED SIGNATURES, AND TOLERANCE ANALYSIS

The numerical feasibility of the proposed validation scheme is evaluated with General Particle Tracer (GPT) [17, 18]. GPT is used to track the relativistic electron bunch from the source to the spectrometer, while the laser–beam interaction is represented by an externally prescribed focused electromagnetic field in the co-propagating section. The purpose of the simulation is to determine whether the regime transition predicted by Eqs. (2) and (3) remains observable in the final energy spectrum under realistic beamline conditions.

Table 1: Key Parameter Settings for Each Component

Parameter	Value
RPL Pulse Parameters	
Wavelength (λ)	800 nm
Pulse duration (τ_L, FWHM)	200 fs
Critical focal waist radius (w_0^{crit})	5 µm
Normalized vector potential (a_0)	0.281
Pulse energy	8 mJ
Distance from photocathode to laser focus	0.53 m
Time delay relative to the beam	70 fs
Electron Beam and RF Gun Parameters	
Beam charge (Q_b)	8 fC
RF gun accelerating field amplitude (E_{RF})	95 MV/m
RF gun frequency ($\omega_{\mathrm{RF}}/2\pi$)	2856 MHz
RF gun cavity structure	1.6-cell
Output kinetic energy from RF gun (E_k)	4.561 MeV
Thermal emittance	10.8 nm rad
Drive Laser Parameters	
Laser pulse duration	200 fs
Laser spot radius on cathode	30 µm
Temporal profile	Gaussian
Spatial profile	Gaussian
Solenoid Parameters	
Solenoid position	0.15 m
Magnetic field strength	0.315 T

The simulation workflow follows the validation logic introduced above. First, the laser-off case is tracked to establish the unperturbed downstream energy spectrum. Then the laser-on case is simulated for waist values w_0. In this way, the numerical study separates the waist-driven regime transition from additional asymmetries introduced by experiment imperfections.

The predicted signatures can be summarized in three regimes under a fixed time-of-arrival delay. For $w_0 \gg w_0^{\mathrm{crit}}$, the interaction remains well inside the multi-cycle regime, and the downstream spectrum is expected to exhibit a comparatively smooth and one-sided broadening, consistent with the cycle-averaged ponderomotive model, with the shift arising from time delay. For $w_0 \sim w_0^{\mathrm{crit}}$, the spectral response becomes more sensitive to the finite interaction length and to the detailed field evolution near focus, marking the transition region in which the cycle-averaged approximation becomes marginal. For $w_0 < w_0^{\mathrm{crit}}$, the theory predicts that the cycle-averaged description should lose reliability, and the spectrum is therefore expected to deviate from the trend of one-sided broadening and to show stronger sensitivity to phase-dependent and non-ideal effects [1].

Within this framework, the primary validation observable is the waist dependence of the spectral broadening $\Delta\sigma_E$ and of the associated spectral reshaping. A successful validation is defined by the consistency between the measured waist-dependent spectral evolution and the regime structure predicted by the critical-waist theory. The centroid shift ΔE_c is retained as a secondary quantity, mainly because it is sensitive to timing offset and asymmetric overlap and therefore provides a useful diagnostic of non-ideal operation. Fig. 2 shows the beam energy spectrum distributions under different light waist conditions in a simulation of real-world conditions. Simulation results indicate that the critical size plays a crucial role in sustaining the ponderomotive effect. At the critical size, beam energy dissipation increases significantly, and carrier-phase modulation becomes dominant, disrupting the single acceleration or deceleration mechanism characteristic of the ponderomotive regime. By adjusting the laser waist in experiments, the aforementioned theoretical mechanism can be verified.

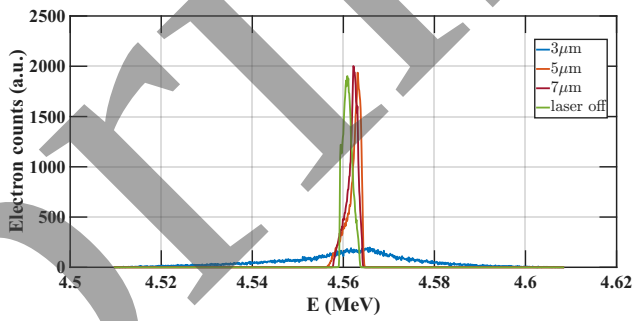

Figure 2: The effect of different laser beam sizes on the electron energy spectrum. 5 µm is the critical size at which ponderomotive effects occur at this energy, while 3 µm significantly suppresses these effects.

CONCLUSION

A practical validation scheme for relativistic ponderomotive dynamics has been developed by translating the previously derived longitudinal ponderomotive-force model into a realistic MeV electron-beam experiment. The central physical concept of the present study is the critical laser waist w_0^{crit}, which follows from the effective-cycle analysis and defines the transition between the cycle-averaged regime and the near-critical interaction regime.

A corresponding beamline configuration has been defined and evaluated with GPT-based simulations. The results indicate that the most robust validation signatures under nominal conditions are laser-induced spectral broadening and symmetric spectral reshaping, while centroid shift is mainly sensitive to effects such as timing offset and imperfect overlap. These results provide a concrete basis for future beam tests and define the operating window for experimental validation of the critical-waist picture in relativistic ponderomotive dynamics.

REFERENCES

[1] J. Zhang *et al.*, "Relativistic ponderomotive dynamics and multiscale modulation mechanisms in optical field compression of electron beams", *Phys. Rev. Accel. Beams*, vol. 29, no. 4, p. 044401, 2026. doi:10.1103/w7jl-pcy2

[2] B. Quesnel and P. Mora, "Theory and simulation of the interaction of ultraintense laser pulses with electrons in vacuum", *Phys. Rev. E*, vol. 58, no. 3, pp. 3719–3732, 1998. doi:10.1103/PhysRevE.58.3719

[3] I. Y. Dodin and N. J. Fisch, "Positive and negative effective mass of classical particles in oscillatory and static fields", *Phys. Rev. E*, vol. 77, p. 036402, 2008. doi:10.1103/PhysRevE.77.036402

[4] L. Serafini and J. B. Rosenzweig, "Envelope analysis of intense relativistic quasilaminar beams in rf photoinjectors: a theory of emittance compensation", *Phys. Rev. E*, vol. 55, no. 6, pp. 7565–7590, 1997. doi:10.1103/PhysRevE.55.7565

[5] H. Chen *et al.*, "Commissioning the photoinjector of a gamma-ray light source", *Phys. Rev. Accel. Beams*, vol. 22, p. 053403, 2019. doi:10.1103/PhysRevAccelBeams.22.053403

[6] P. H. Bucksbaum, M. Bashkansky, and T. J. McIlrath, "Scattering of electrons by intense coherent light", *Phys. Rev. Lett.*, vol. 58, no. 4, pp. 349–352, 1987. doi:10.1103/PhysRevLett.58.349

[7] J. J. Axelrod, S. L. Campbell, O. Schwartz, C. Turnbaugh, R. M. Glaeser, and H. Müller, "Observation of the relativistic reversal of the ponderomotive potential", *Phys. Rev. Lett.*, vol. 124, p. 174801, 2020. doi:10.1103/PhysRevLett.124.174801

[8] A. V. Gaponov and M. A. Miller, "Potential wells for charged particles in a high-frequency electromagnetic field", *Sov. Phys. JETP*, vol. 7, no. 1, pp. 168–169, 1958.

[9] T. W. B. Kibble, "Refraction of electron beams by intense electromagnetic waves", *Phys. Rev. Lett.*, vol. 16, no. 23, pp. 1054–1056, 1966. doi:10.1103/PhysRevLett.16.1054

[10] A. J. Brizard and T. S. Hahm, "Foundations of nonlinear gyrokinetic theory", *Rev. Mod. Phys.*, vol. 79, no. 2, pp. 421–468, 2007. doi:10.1103/RevModPhys.79.421

[11] R. B. Palmer, "Interaction of relativistic particles and free electromagnetic waves in the presence of a static helical magnet", *J. Appl. Phys.*, vol. 43, no. 7, pp. 3014–3023, 1972. doi:10.1063/1.1661650

[12] T. Xu, F. Ji, C. J. R. Duncan, S. P. Weathersby, and R. J. England, "Calculation of rf-induced temporal jitter in ultrafast electron diffraction", *Phys. Rev. Accel. Beams*, vol. 28, p. 024001, 2025. doi:10.1103/PhysRevAccelBeams.28.024001

[13] M. Lax, W. H. Louisell, and W. B. McKnight, "From maxwell to paraxial wave optics", *Phys. Rev. A*, vol. 11, no. 4, pp. 1365–1370, 1975. doi:10.1103/PhysRevA.11.1365

[14] L. W. Davis, "Theory of electromagnetic beams", *Phys. Rev. A*, vol. 19, no. 3, pp. 1177–1179, 1979. doi:10.1103/PhysRevA.19.1177

[15] G. P. Agrawal and D. N. Pattanayak, "Free-space wave propagation beyond the paraxial approximation", *Phys. Rev. A*, vol. 27, no. 4, pp. 1693–1695, 1983. doi:10.1103/PhysRevA.27.1693

[16] S. A. Self, "Focusing of spherical gaussian beams", *Appl. Opt.*, vol. 22, no. 5, pp. 658–661, 1983. doi:10.1364/AO.22.000658

[17] M. J. de Loos and S. B. van der Geer, "General particle tracer: a new 3D code for accelerator and beamline design", in *Proc. EPAC'96*, Sitges, Spain, Jun. 1996, pp. 1241–1243.

[18] S. B. van der Geer and M. J. de Loos, "The general particle tracer code: design, implementation and application", Ph.D. thesis, Technische Universiteit Eindhoven, Eindhoven, The Netherlands, 2001. doi:10.6100/IR542912